

# Mechanisms of scattering of surface electrons in topological insulators

Cite as: Low Temp. Phys. **45**, 118 (2019); <https://doi.org/10.1063/1.5082322>

Published Online: 22 January 2019

Yu. V. Toporov, and A. A. Kordyuk



View Online



Export Citation



CrossMark

## ARTICLES YOU MAY BE INTERESTED IN

[Deformation-induced phase transition in Weyl semimetals: pseudo-field origin of effect](#)

Low Temperature Physics **45**, 107 (2019); <https://doi.org/10.1063/1.5082320>

[Spin-phonon interaction in transition-metal difluoride antiferromagnets: Theory and experiment](#)

Low Temperature Physics **45**, 78 (2019); <https://doi.org/10.1063/1.5082316>

[Dissipative motion of vortices in spatially inhomogeneous Bose-Einstein condensates](#)

Low Temperature Physics **45**, 67 (2019); <https://doi.org/10.1063/1.5082312>



LOW TEMPERATURE TECHNIQUES  
OPTICAL CAVITY PHYSICS  
MITIGATING THERMAL  
& VIBRATIONAL NOISE

**DOWNLOAD THE WHITE PAPER**

[downloads.montainstruments.com/optical\\_cavities](https://downloads.montainstruments.com/optical_cavities)

MONTANA INSTRUMENTS  
COLD SCIENCE MADE SIMPLE

# Mechanisms of scattering of surface electrons in topological insulators

Cite as: *Fiz. Nizk. Temp.* **45**, 134–139 (January 2019); doi: [10.1063/1.5082322](https://doi.org/10.1063/1.5082322)

Submitted: 20 November 2018



View Online



Export Citation



CrossMark

Yu. V. Toporov<sup>1,a)</sup> and A. A. Kordyuk<sup>2,3,b)</sup>

## AFFILIATIONS

<sup>1</sup>Taras Shevchenko National University of Kyiv, 60 Volodymyrska Street, Kyiv city, Ukraine, 01033

<sup>2</sup>Kyiv Academic University, 36 Vernadskyi blvd., Kyiv, Ukraine, 03142

<sup>3</sup>G.V. Kurdyumov Institute for Metal Physics of the National Academy of Science of Ukraine, 36 Vernadskyi blvd., Kyiv, Ukraine, 03142

<sup>a)</sup>Email: [toporov94@gmail.com](mailto:toporov94@gmail.com)

<sup>b)</sup>Email: [kordyuk@gmail.com](mailto:kordyuk@gmail.com)

## ABSTRACT

A unique feature of topological insulators is the presence of electronic topologically protected quasiparticle surface states that are exceptionally resistant to impurities; however, the scattering spectrum of these surface quasiparticles is poorly studied. The purpose of this study is to determine the structure of the surface state eigenenergy by analyzing photoemission spectra. In particular, the broadening of these states as a function of the binding energy in  $\text{Bi}_2\text{Se}_3$  and  $\text{Bi}_2\text{Te}_2\text{Se}$  — the most extensively studied topological insulators, has been studied in detail. The revealed stepped structure of broadening allowed us to distinguish the contributions of elastic and inelastic interband scattering (surface–bulk) to the quasiparticle eigenenergy and to show that it is comparable with elastic intraband scattering.

Published under license by AIP Publishing. <https://doi.org/10.1063/1.5082322>

## INTRODUCTION

Topologically protected states on the surface of bulk insulators are possible due to a combination of spin-orbit interaction and time inversion symmetry.<sup>1</sup> The existence of such states allows the topological insulator to conduct current on the surface, while remaining a dielectric in the bulk. In addition, the surface remains metallic even with very strong disordering, for example, during charge carrier scattering by impurities and defects. This was experimentally demonstrated by scanning tunneling spectroscopy<sup>2</sup> and angle-resolved photoemission spectroscopy (ARPES),<sup>3,4</sup> which is perfect for studying surface states.<sup>5</sup> Topological invariance can be used to create quantum computers, especially those based on Majorana fermions, which are extremely resistant to noise and environmental effects, and could be used for reliable storage and transmission of information.<sup>1</sup>

It is obvious that the basis for the effective use of topological insulators should be the understanding of the scattering mechanisms of these “topologically protected” surface states. And one would expect that these mechanisms would be rather quickly identified in direct ARPES experiments,<sup>5</sup> for

example, by analyzing the structure of the quasiparticle eigenenergy, as it was done in the case of superconducting cuprates.<sup>6,7</sup> However, only a few studies on the eigenenergy structure in topological insulators have been published,<sup>8</sup> due to low attenuation (the width of spectra is proportional to the attenuation and is comparable to the experimental resolution), and the influence of bulk states that complicate spectral analysis.<sup>5</sup>

Surface states have a long lifetime, since they are spin-polarized.<sup>1</sup> The electron spin should change its direction, in order for an electron to move to another surface state. The probability of this process is very small. On the other hand, nothing prevents electron scattering to the bulk state where the topological protection is absent. However, the surface and bulk states in the crystal are spatially separated, and the overlap region is small. The use of a detailed analysis of the ARPES spectra makes it possible to reveal the degree of influence of these two states onto each other by estimating the relative probability of interband and intraband transitions.

In this study, the use of ARPES spectra with improved statistics, allowed us to study the correlation of the surface and bulk states of bismuth selenide  $\text{Bi}_2\text{Se}_3$  and a compound

containing tellurium  $\text{Bi}_2\text{Te}_2\text{Se}$ , by investigating the structure of quasiparticle scattering. The contributions of elastic and inelastic scattering to quasiparticle eigenenergy, which determine the lifetime of topological states, are found.

## EXPERIMENTAL PROCEDURE

The ARPES spectrum reflects the probability of finding an electron with an energy  $\omega$  and a momentum  $\mathbf{k}$  in the crystal, as well as its transfer to an excited state. The first process is determined by the density of the filled states, or by the spectral function multiplied by the Fermi distribution:  $A(\omega, \mathbf{k})f(\omega)$ . The second process is determined by the probability of photon absorption or a direct transition to the free level (it defines the “matrix elements”  $M(\hbar\nu, n, \mathbf{k})$  in the three-step model of photoemission). Thus, the ARPES spectrum structure, which consists of  $n$  bands, in coordinates  $(\omega, \mathbf{k})$  looks like:

$$\text{ARPES}(\omega, \mathbf{k}) \propto \sum_n M(\hbar\nu, n, \mathbf{k}) A(\omega, \mathbf{k}) f(\omega). \quad (1)$$

The spectral function  $A(\omega, \mathbf{k})$  contains information about the electronic subsystem properties and obtaining it is the main purpose of photoemission studies. Its structure can be represented as<sup>9,10</sup>

$$A(\omega, \mathbf{k}) = -\frac{1}{\pi} \frac{\sum''(\omega, \mathbf{k})}{(\omega - \epsilon(\mathbf{k}) - \sum'(\omega, \mathbf{k}))^2 + (\sum''(\omega, \mathbf{k}))^2}. \quad (2)$$

Here  $\epsilon(\mathbf{k})$  is the “bare” dispersion, which is determined by the elastic interaction of electrons with the crystal lattice, and the complex eigenenergy  $\Sigma$  is determined by the interaction of electrons with other electrons or other degrees of freedom in a crystal (phonons, spin fluctuations) and, thus, contains all the information on the properties of single-particle excitations in correlated systems. The real part determines the dispersion of particles, and the imaginary part determines their attenuation or, in other words, lifetime.

The dependence of the imaginary part  $\Sigma = \Sigma' + i\Sigma''$  on energy is the subject of the research in this article. Fig. 1 illustrates how these values can be determined from the experimental spectrum.<sup>5</sup>

In order to obtain the dependence  $\Sigma''$ , we analyzed the momentum distribution curves (MDC),<sup>10</sup> an example of which is shown in Fig. 1.<sup>5,11</sup> Each MDC function from the Fermi energy to the Dirac point was approximated by a Lorentzian whose peak positions and half-widths correspond to the dependences of dispersion and quasiparticle attenuation on quasiparticle energy.

An example of the momentum distribution curve  $\text{MDC}(k)$  is shown in Fig. 2. The approximating function  $\text{MDC\_fit}(k)$  components are illustrated by dotted lines:

$$\begin{aligned} \text{MDC\_fit}(k) &= Q(k) + L1(k) + L2(k) \\ &= (Q_1 k^2 + Q_0) + \frac{A_1 W_1^2}{(k - k_1)^2 + W_1^2} + \frac{A_2 W_2^2}{(k - k_2)^2 + W_2^2}, \end{aligned} \quad (3)$$

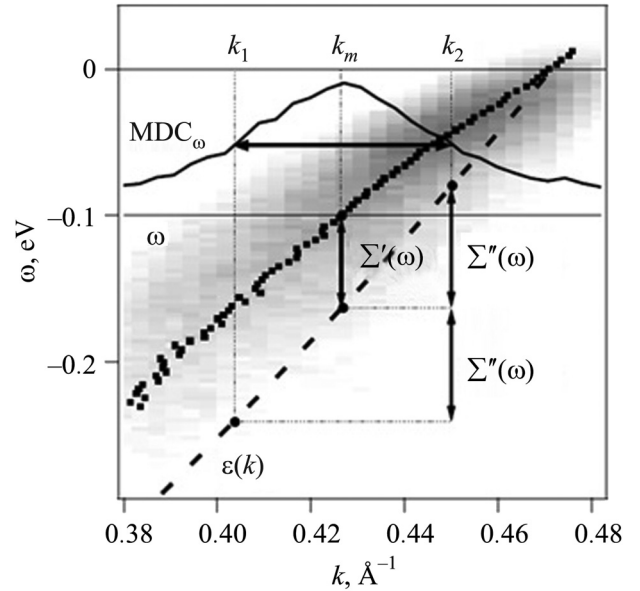


FIG. 1. The difference between “bare” and experimental dispersion. The relationship between MDC and eigenenergy components is also shown.<sup>5,11</sup>

where  $Q_0, Q_1, A_1, A_2, W_1, W_2, k_1$ , and  $k_2$  are the approximation parameters.

The approximating function is the simplest, physically valid model of photoemission spectra<sup>5,11</sup> and consists of three terms containing the minimum required set of parameters. The first term  $Q(k) = (Q_1 k^2 + Q_0)$  determines the background. A quadratic function is chosen here, since the background should have a symmetric impact on electrons with pulses of opposite signs. The second term  $L1(k)$  is the Lorentzian of the band of surface states, whose parameters  $k_1$  and  $W_1$  determine

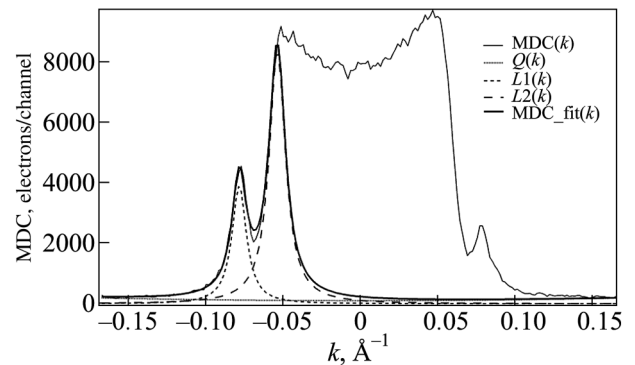


FIG. 2. Momentum distribution curve and its approximating function components.

the renormalized dispersion of surface states and the imaginary portion of the eigenenergy, respectively. The third term  $L_2(k)$  is also represented by a Lorentzian and is used to take into account the influence of the band of bulk states. Since the purpose of this work was the selection and subsequent analysis of  $W_1(\omega)$ , the structure of the approximating function was optimized precisely for the determination of this parameter, and the role of the remaining terms was to improve the accuracy of approximation in the vicinity of the peak of surface states. In particular, the difference in  $W_1$  values with and without consideration of the third term is approximately 8%; however, the difference in the case when the second term is considered in the form of a Lorentzian or, for example, a Gaussian is less than 2%, which is sufficient for reliable identification of the features discussed in this article. Thus, although the sensitivity of  $W_1(\omega)$  to variation of parameters is insignificant, their consideration is necessary for the accurate determination of surface state parameters.

The dependence of  $\Sigma''$  on energy is based on the following equation:

$$\Sigma'' = W_1(\omega)v_F. \quad (4)$$

Here  $W_1(\omega)$  is the dependence obtained by approximating the experimental MDC to Eq. (3),  $v_F$  is the Fermi velocity (the derivative of the energy with respect to the momentum, which is found by approximating the dispersion curve by a polynomial).

## RESULTS AND DISCUSSION

Figure 3 shows the ARPES spectra that were analyzed in this study. All spectra were obtained on a BESSY synchrotron at stations "1<sup>2</sup>" and "1<sup>3</sup>".<sup>8,12,13</sup>

The spectra demonstrate branches of surface states and bands of bulk states between them, and their influence is studied in this article. The band of bulk states is almost invisible in Fig. 3(c) due to the influence of matrix elements.

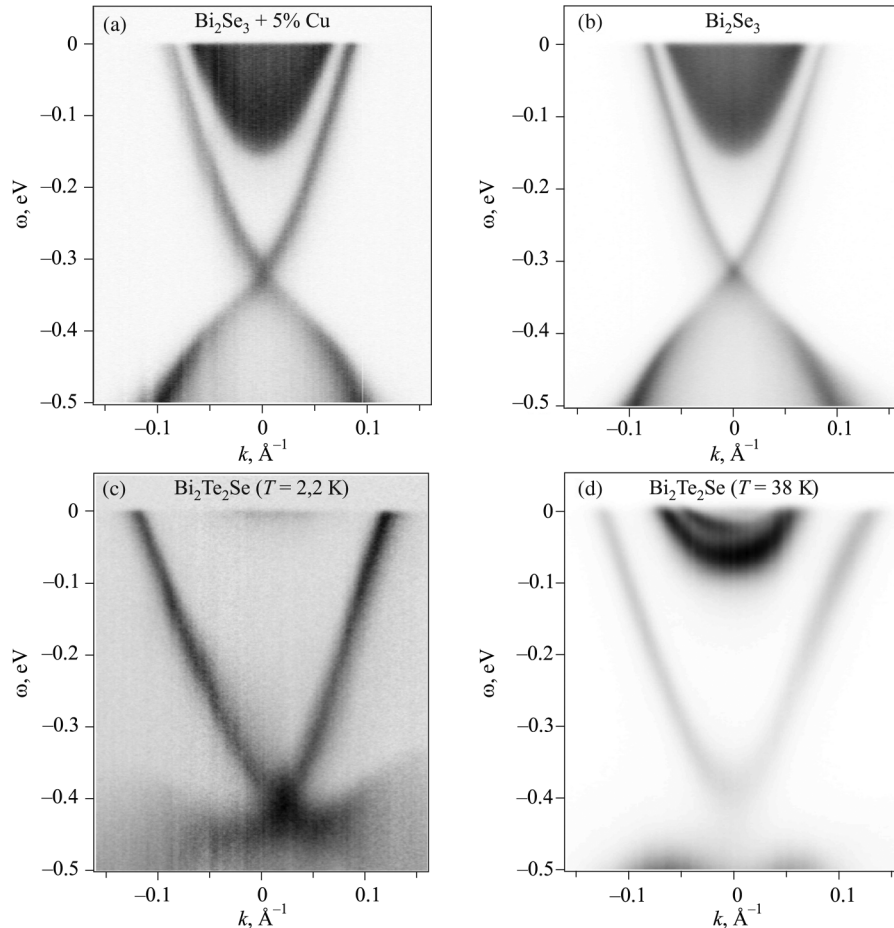


FIG. 3. Typical ARPES spectra of surface states in topological insulators.

Dispersion dependences obtained after approximation are shown in Fig. 4. It can be seen that the dispersions of the two topological insulators differ significantly. This is associated with the different concentration of surface electrons.

Figure 5 shows the quasiparticle attenuation curve  $\Sigma''(\omega)$  obtained from the analysis of the first spectrum [Fig. 3(a)]. The graph was preliminarily smoothed in order to highlight the characteristic areas. Two characteristic steps can be distinguished, which apparently correspond to the boundaries of two contributions to the quasiparticle attenuation, which occurs due to both intraband (surface-surface) and inter-band (surface-bulk) scattering of surface quasiparticles by impurities, phonons, and as a result of electron-electron interaction. The corresponding contributions are indicated in Fig. 5.

Scattering by impurities is proportional to the density of electronic states, therefore, the first step in the scattering (1 in Fig. 5) can be associated only with the edge of the bulk conduction band and, accordingly, is described by the  $\Sigma_{\text{imp}}^b$  dependence.

The electron-phonon interaction spectrum is limited by the Debye frequency,<sup>14</sup> therefore, its contribution should also have the shape of a step:  $\Sigma_{\text{ph}}^b$  will be the convolution of the phonon spectrum and the density of states of the bulk band and, therefore, the onset of absorption will be shifted in energy by the Debye frequency, which explains the second step (2 in Fig. 5). Since the phonon spectrum has strongly pronounced peaks corresponding to optical phonons, this structure is expected to appear during attenuation as well. However, better statistics are required to establish this correspondence.

The remaining contributions to the damping are associated with electron-electron scattering, which leads to a quadratic dependence  $\Sigma''(\omega)$ , so the sum  $\Sigma_{\text{el}}^s + \Sigma_{\text{ph}}^s + \Sigma_{\text{el}}^b$  can be approximated by a quadratic function, as shown in Fig. 5.

The spectra of the other samples, which are shown in Fig. 3, were analyzed to confirm the assumption about the origin of the steps on the  $\Sigma''(\omega)$  graph. The quasiparticle attenuation curves for  $\text{Bi}_2\text{Se}_3$  and  $\text{Bi}_2\text{Te}_2\text{Se}$  are presented in Fig. 6.

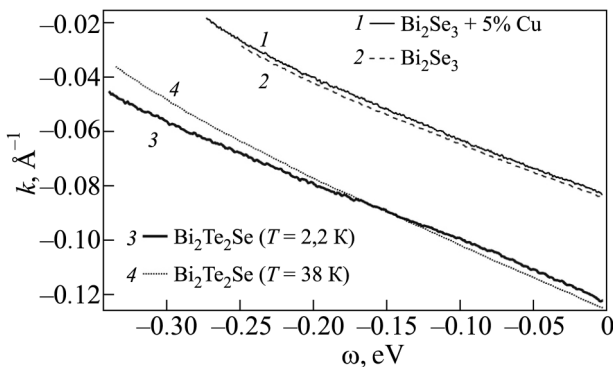


FIG. 4. Dispersion dependences of topological insulators.

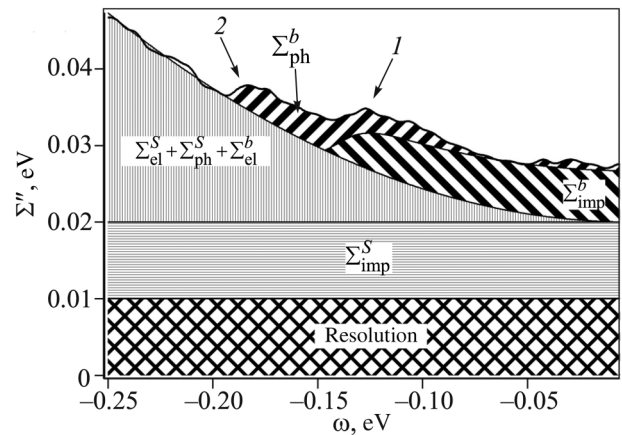


FIG. 5. Quasiparticle scattering components for the first spectrum. Scattering of surface electrons: by phonons into a bulk state  $\Sigma_{\text{ph}}^b$ , by impurities into a bulk state  $\Sigma_{\text{imp}}^b$ , by electrons into surface and bulk states and by phonons into a surface state  $\Sigma_{\text{el}}^s + \Sigma_{\text{ph}}^s + \Sigma_{\text{el}}^b$ , by impurities into a surface state  $\Sigma_{\text{imp}}^s$ , resolution of the instrument (resolution).

The assumption about the origin of the steps was confirmed for bismuth selenide (Fig. 6, curves a and b), and the shift of the steps was associated with a change in the chemical potential due to the doping of the first sample with

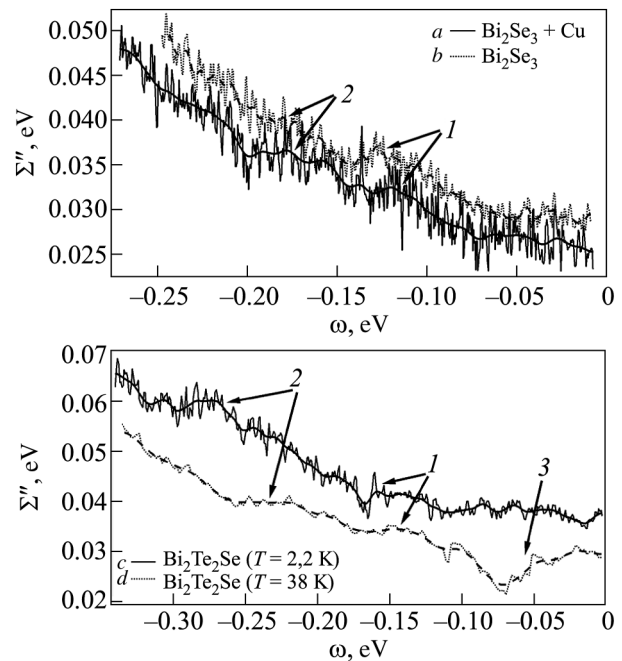


FIG. 6. Quasiparticle attenuation curves  $\Sigma''(\omega)$  for  $\text{Bi}_2\text{Se}_3$  (curves a and b) and  $\text{Bi}_2\text{Te}_2\text{Se}$  (curves c and d).



copper (Fig. 6, curve *a*). This small shift, while maintaining the general shape of the dependence, confirms the fact that the scattering pattern does not change with doping.

Differences between the quasiparticle scattering curves are more pronounced for Bi<sub>2</sub>Te<sub>2</sub>Se. The measurements were carried out on the same sample at different times and under different conditions. A two-dimensional electron gas with surface degradation is formed on the surface of these compounds over time.<sup>4,15</sup> The result of the occurrence of a two-dimensional electron gas is shown in Fig. 3(d) as a parabolic dispersion over bulk states. This effect can be observed on the quasiparticle scattering curve as an increase in  $\Sigma''$  near the Fermi point (3 in Fig. 6, curve *d*), and is the result of the scattering of surface electrons by phonons into the bulk and surface states of a two-dimensional electron gas.

Step 1, in the same manner as for Bi<sub>2</sub>Se<sub>3</sub>, is explained by scattering into a bulk state by impurities. Phonon interaction is a convolution of the phonon spectrum and the density of electronic states; therefore, in this case, the onset of attenuation shifts by 0.1 eV to the left compared to step 1 (the second peak shifts by  $-0.22$  eV), which is the characteristic phonon energy. The curve *c* (second step  $\omega = -0.30$  eV) in Fig. 6 is not associated with phonon interaction (the distance to the second step is more than 0.15 eV), since this energy exceeds the possible energy of phonons. The explanation of this feature requires further research.

## CONCLUSION

The use of an improved procedure for approximating ARPES spectra demonstrated that the lifetime of surface topological states in topological insulators based on Bi<sub>2</sub>Se<sub>3</sub> and Bi<sub>2</sub>Te<sub>2</sub>Se correlates with the density of bulk electronic states and the phonon spectrum. Namely, the appearance of steps is associated with the scattering of surface electrons by impurities and phonons into bulk states. It can also be argued

that both interband contributions are comparable to the elastic intraband scattering of surface quasiparticles.

## REFERENCES

- <sup>1</sup>M. Z. Hasan and C. L. Kane, *Rev. Mod. Phys.* **82**, 3045 (2010).
- <sup>2</sup>P. Roushan, J. Seo, C. V. Parker, Y. S. Hor, D. Hsieh, D. Qian, A. Richardella, M. Z. Hasan, R. J. Cava, and A. Yazdani, *Nature* **460**, 1106 (2009).
- <sup>3</sup>D. Hsieh, Y. Xia, D. Qian, L. Wray, J. H. Dil, F. Meier, J. Osterwalder, L. Patthey, J. G. Checkelsky, N. P. Ong, A. V. Fedorov, H. Lin, A. Bansil, D. Grauer, Y. S. Hor, R. J. Cava, and M. Z. Hasan, *Nature* **460**, 1101 (2009).
- <sup>4</sup>M. Bianchi, D. Guan, S. Bao, J. Mi, B. B. Iversen, P. D. C. King, and P. Hofmann, *Nat. Commun.* **1**, 128 (2010).
- <sup>5</sup>A. A. Kordyuk, *Fiz. Nizk. Temp.* **40**, 375 (2014) [*Low Temp. Phys.* **40**, 286 (2014)].
- <sup>6</sup>A. A. Kordyuk and S. V. Borisenko, *Fiz. Nizk. Temp.* **32**, 401 (2006) [*Low Temp. Phys.* **32**, 298 (2006)].
- <sup>7</sup>A. A. Kordyuk, V. B. Zabolotnyy, D. V. Evtushinsky, D. S. Inosov, T. K. Kim, B. Büchner, and S. V. Borisenko, *Eur. Phys. J. Special Topics* **188**, 153 (2010).
- <sup>8</sup>A. A. Kordyuk, V. B. Zabolotnyy, D. V. Evtushinsky, T. K. Kim, B. Büchner, I. V. Plushchay, H. Berger, and S. V. Borisenko, *Phys. Rev. B* **85**, 075414 (2012).
- <sup>9</sup>A. A. Kordyuk, S. V. Borisenko, A. Koitzsch, J. Fink, M. Knupfer, and H. Berger, *Phys. Rev. B* **71**, 214513 (2005).
- <sup>10</sup>T. Valla, A. V. Fedorov, P. D. Johnson, B. O. Wells, S. L. Hulbert, Q. Li, G. D. Gu, and N. Koshizuka, *Science* **285**, 2110 (1999).
- <sup>11</sup>D. V. Evtushinsky, A. A. Kordyuk, S. V. Borisenko, V. B. Zabolotnyy, M. Knupfer, J. Fink, B. Büchner, A. V. Pan, A. Erb, C. T. Lin, and H. Berger, *Phys. Rev. B* **74**, 172509 (2006).
- <sup>12</sup>A. A. Kordyuk, T. K. Kim, V. B. Zabolotnyy, D. V. Evtushinsky, M. Bauch, C. Hess, B. Büchner, H. Berger, and S. V. Borisenko, *Phys. Rev. B* **83**, 081303 (2011).
- <sup>13</sup>S. V. Borisenko, V. B. Zabolotnyy, A. A. Kordyuk, D. V. Evtushinsky, T. K. Kim, E. Carleschi, B. P. Doyle, R. Fittipaldi, M. Cuoco, A. Vecchione, and H. Berger, *J. Vis. Exp.* **68**, e50129 (2012).
- <sup>14</sup>R. C. Hatch, M. Bianchi, D. Guan, S. Bao, J. Mi, B. B. Iversen, L. Nilsson, L. Hornekaer, and P. Hofmann, *Phys. Rev. B* **83**, 241303 (2011).
- <sup>15</sup>M. S. Bahramy, P. King, A. de la Torre, J. Chang, M. Shi, L. Patthey, G. Balakrishnan, P. Hofmann, R. Arita, N. Nagaosa, and F. Baumberger, *Nat. Commun.* **3**, 1159 (2012).

Translated by AIP Author Services.